Multivesicular Release at Single Functional Synaptic Sites in Cerebellar Stellate and Basket Cells

Céline Auger, Satoru Kondo, Alain Marty

The Journal of Neuroscience, June 15, 1998, *18*(12):4532–4547

Multivesicular Release at Single Functional Synaptic Sites in Cerebellar Stellate and Basket Cells

Céline Auger, Satoru Kondo, and Alain Marty

Arbeitsgruppe Zelluläre Neurobiologie, Max-Planck-Institut für biophysikalische Chemie, 37077, Göttingen, Germany

The purpose of the present work was to test the hypothesis that no more than one vesicle of transmitter can be liberated by an action potential at a single release site. Spontaneous and evoked IPSCs were recorded from interneurons in the molecular layer of cerebellar slices. Evoked IPSCs were obtained using either extracellular stimulation or paired recordings of presynaptic and postsynaptic neurons. Connections were identified as single-site synapses when evoked current amplitudes could be grouped into one peak that was well separated from the background noise. Peak amplitudes ranged from 30 to 298 pA. Reducing the release probability by lowering the external Ca^{2+} concentration or adding Cd^{2+} failed to reveal smaller quantal components. Some spontaneous IPSCs (1.4–2.4%) and IPSCs evoked at single-site synapses (2–6%) were followed within <5 msec by a secondary IPSC that could not be accounted for by random occurrence of background IPSCs. Nonlinear summation of closely timed events indicated that they involved activation of a common set of receptors and therefore that several vesicles could be released at the same release site by one action potential. An average receptor occupancy of 0.70 was calculated after single release events. At some single-site connections, two closely spaced amplitude peaks were resolved, presumably reflecting single and double vesicular release. Consistent with multivesicular release, kinetics of onset, decay, and latency were correlated to IPSC amplitude. We conclude that the one-site, one-vesicle hypothesis does not hold at interneuron–interneuron synapses.

Key words: synaptic transmission; cerebellum; GABA; stellate cells; basket cells; quantal analysis; vesicular release

Synaptic signals fluctuate because of the random occurrence of discrete units ("quanta") reflecting the exocytosis of single presynaptic vesicles (Katz, 1969). At central synapses, amplitude histograms of evoked synaptic potentials have been fitted with binomial distributions, and the number of peaks is believed to correspond to the number of release sites (Redman, 1990). Such a correspondence requires that a single release site contributes at most one quantum, either because some intrinsic limitation prevents the release of more than one vesicle (Triller and Korn, 1982) or because the postsynaptic receptors are close to saturation so that simultaneous release events are indistinguishable from singular events (Redman, 1990). The original formulation of the one-site, one-quantum hypothesis and of its more restrictive variant the one-site, one-vesicle hypothesis were based, however, on model-dependent interpretations of amplitude distributions at multisite connections. Such methods are indirect and have been subjected to criticism (Clements, 1991; Bekkers, 1994).

Recently, more direct evidence started to accumulate indicating that indeed, single-site signals are limited to one quantum. At excitatory synapses between CA3 pyramidal cells and interneurons in the hippocampus, morphological evidence indicates predominantly single-site contacts, whereas evoked postsynaptic signals display a Gaussian amplitude distribution (Gulyàs et al., 1993; Arancio et al., 1994). Likewise, some mossy fiber–granule cell synapses in the cerebellum have single-Gaussian amplitude distributions and behave as expected for single-site synapses when the the external Ca^{2+} concentration is lowered (Silver et al., 1996). The striking absence of double-sized events at single-site synapses (Gulyàs et al., 1993; Arancio et al., 1994; Silver et al., 1996) leaves little doubt about the validity of the one-site, one-quantum hypothesis. The question that remains open, however, is whether the lack of a secondary peak reflects inhibition of multiple release (one-site, one-vesicle hypothesis) or saturation of postsynaptic receptors.

Tong and Jahr (1994) and Scanziani et al. (1997) reported a differential block of EPSCs by low-affinity competitive antagonists under normal and high release probability conditions, indicating that postsynaptic receptors are exposed to a higher or more prolonged neurotransmitter concentration in the latter case. Moreover, the time course of synaptic currents is prolonged under high release conditions in certain synapses (for review, see Barbour and Häusser, 1997). Although these observations can be interpreted as indicating multivesicular release (Tong and Jahr, 1994), it was recently pointed out that they are equally well explained by cross-talk between neighboring synapses (Barbour and Häusser, 1997; Scanziani et al., 1997).

The present work examines the question of multivesicular release by taking advantage of the properties of interneuron–interneuron synapses in the molecular layer of the cerebellum. At these synapses, miniature currents are very large, with a mean of 140 pA at −60 mV under symmetrical Cl^- concentration conditions (Llano and Gerschenfeld, 1993). Furthermore, the mean size of spontaneous IPSCs recorded in control solution is similar

Received Jan. 26, 1998; revised March 18, 1998; accepted April 6, 1998.

This work was supported by a fellowship from the French Ministère de la Recherche et de la Technologie (C.A.), by a Human Frontier Science Program fellowship (S.K.), and by the Deutsche Forschungsgemeinschaft (SFB 406). We thank C. Pouzat and P. Vincent for sharing analysis software, and L. Forti and I. Llano for comments on this manuscript.

Correspondence should be addressed to Dr. A. Marty, Arbeitsgruppe Zelluläre Neurobiologie, Max-Planck-Institut für biophysikalische Chemie, 37077, Göttingen, Germany.

Dr. Kondo's present address: Laboratory for Neural Circuit, Bio-Mimetic Control Research Center, RIKEN, Anagahora, Shimoshidami, Moriyama-ku, Nagoya, Aichi 463, Japan.

to that of miniature IPSCs (mIPSCs), suggesting that some connections involve single release sites (Llano and Gerschenfeld, 1993). We report here that multivesicular release occurs in this preparation.

MATERIALS AND METHODS

Slice preparation. Cerebellar slices were prepared as described previously (Llano et al., 1991). Briefly, rats (12- to 16-d-old) were killed by decapitation under anesthesia with Metofane. The vermis of the cerebellum was quickly removed and placed in ice-cold solution. Slices, 180-μm-thick, were cut parallel to the sagittal plane. They were kept in a vessel bubbled with 95% O_2 and 5% CO_2 at 33°C for 1–6 hr before recording.

Patch-clamp recordings. Patch-clamp recordings were made from inhibitory interneurons (stellate or basket cells) of the molecular layer of the cerebellum. The cells were differentiated from migrating granule cells or glia by the size of their soma (~8 μm). The identification was confirmed by the observation of spikes in the cell-attached mode and of spontaneous synaptic activity as well as of voltage-dependent Na^+ currents after breaking into the cell. The tight-seal whole-cell recording technique was used in all cases to record postsynaptic IPSCs. When filled with internal saline, the recording pipettes had a resistance of 3–5 MΩ. The internal solution used was either a K^+- or Cs^+-based solution. The K^+-based solution contained (in mM): 150 KCl, 4.6 $MgCl_2$, 0.1 $CaCl_2$, 1 EGTA, 10 K-HEPES, 0.4 NaGTP, and 4 NaATP, or alternatively 120 KCl, 4.6 $MgCl_2$, 1 $CaCl_2$, 10 EGTA, 10 K-HEPES, 0.4 NaGTP, and 4 NaATP. The Cs^+-based solution contained (in mM): 124 CsCl, 4.6 $MgCl_2$, 0.1 $CaCl_2$, 1 EGTA, 10 HEPES, 0.4 NaGTP, and 4 NaATP. The holding potential was −60 mV. The mean cell capacitance and uncompensated series resistance were 5.9 ± 1.9 pF and 16.9 ± 7.3 MΩ, respectively. The series resistance was compensated between 50 and 90%.

The bath was perfused continuously at a rate of 1–1.5 ml/min with an external solution of the following composition (in mM): 125 NaCl, 2.5 KCl, 1.25 NaH_2PO_4, 26 $NaHCO_3$, and 10 glucose. In control recordings, the external solution was supplemented with 2 mM $CaCl_2$ and 1 mM $MgCl_2$. This was also the solution used for cutting and keeping the slices. The probability of release was decreased in some experiments by reducing the external Ca^{2+} concentration down to 1.5–1 mM Ca^{2+} and increasing the Mg^{2+} concentration to 1.5–2 mM Mg^{2+}, or by adding 2.5 μM Cd^{2+} to the control solution. The external solution was bubbled continuously with a mixture of 95% O_2 and 5% CO_2 to maintain the pH at 7.4. All experiments were performed at room temperature.

Extracellular stimulation. A presynaptic interneuron was stimulated using an extracellular electrode. The electrode was made of a patch pipette that was filled with extracellular saline and had a resistance of 1–4 MΩ. The ground electrode for the stimulation circuit was made with a platinum wire wrapped around the stimulation electrode. A voltage pulse (1–100 V) was applied through the stimulation electrode for 200–400 μsec. The stimulation electrode was positioned in the molecular layer at the surface of the slice, and stimulus intensity was increased until IPSCs were evoked.

Paired recordings. In paired recordings the electrical activity of the presynaptic interneuron was monitored in the cell-attached mode, whereas postsynaptic signals were obtained using whole-cell recording. Experimental procedures for paired recordings as well as basic properties of IPSCs in 20 connected pairs are described in a separate publication (Kondo and Marty, 1998). In the present paper we show the results of latency analysis using the same recordings as data base.

Analysis of spontaneous IPSCs. Synaptic currents were identified using a detection program, as detailed elsewhere (Vincent and Marty, 1993). Individual synaptic currents were inspected to reject occasional EPSCs, on the basis of their specific kinetic properties (Llano and Gerschenfeld, 1993). Double IPSCs were identified by visual inspection; amplitudes and time intervals for doublets were measured using cursors.

To calculate the distribution of amplitude ratios for consecutive events, A_2/A_1, assuming random superimposition of the events (see Fig. 2*E*), single IPSCs were chosen randomly, and their amplitudes, a_i, were measured. The ratios $r_{i,j} = a_j/a_i$ were formed for all i, j pairs with $i \neq j$. The normalized average time course of all events, $y(t)$, was calculated, with $y(0) = 1$. For a lag δt between two events, first events have decayed to $y(\delta t)$ times their peak when the second event occurs, such that the A_2/A_1 ratio for each i, j doublet (event with index i first) is $(a_i\, y(\delta t) + a_j)/a_i = y(\delta t) + r_{i,j}$.

The distribution of such ratios was calculated for each bin (see Fig. 2*A*), taking as δt the central interval value in the bin, and was normalized to the number of events expected per time interval bin. The components for each of the bins were then added together (see Fig. 2*E*, *dotted curve*).

Analysis of the synaptic responses (extracellular stimulation). For each sweep, IPSCs were detected within a time window of ~3 msec, using a routine with a threshold amplitude of 10 pA written by C. Pouzat in our laboratory. When no IPSC was detected (failures), an amplitude was measured in the same window, at a point determined arbitrarily. As a rule, the amplitude histogram of evoked IPSCs did not overlap significantly with that of the background noise measured in this manner. The average failure sweep did not contain any signal having kinetics similar to that of IPSCs, confirming that events classified as failures did not include undetected IPSCs. If two events occurred within the detection window, only the amplitude corresponding to the larger of the two was registered. The coefficient of variation (CV) was calculated as $CV = (var_{IPSC} - var_{noise})^{1/2}/mean_{IPSC}$, where var_{IPSC} and var_{noise} are the variance of the IPSCs and of background noise, respectively, and $mean_{IPSC}$ is the average amplitude of successful responses. In the figures, background noise histograms and evoked IPSCs histograms are scaled to the same maximum. For the analysis of the kinetics of single and multiple events (see Fig. 8), latencies were measured by hand as the first point of the IPSC that clearly deviated from the baseline current.

Detection of doublets in paired recordings and extracellular stimulation experiments was performed as for spontaneous recordings. However, jitter among IPSC components contributed by different release sites had to be taken into account in the analysis of spontaneous recordings. Therefore a threshold for the minimum time separating two events was taken as 1 or 1.5 msec for the analysis of spontaneous events, depending on the experiment. For analysis of evoked currents, there was no need for such a threshold, because only single-site experiments were examined, and the effective minimum separation between reliably measured doublets was ~0.5 msec.

Statistical test for event pairing. To test whether events were correlated for short time intervals, the number of pairs observed for one interval bin, n_{obs}, was compared with that expected for a Poisson process, n_p, on the basis of the mean event frequency. Typically n_{obs} was larger than n_p, indicating correlation. To evaluate the statistical significance of the difference between n_{obs} and n_p, the probability was calculated to obtain a number of observations equal to or larger than n_{obs}, assuming Poisson statistics with mean n_p. This is:

$$p = 1 - \exp(-n_p) \sum_{n=0}^{n_{obs}-1} n_p{}^n/n!.$$

If p was <0.05 it was considered that there was a significantly larger number of pairs than predicted for a Poisson process.

For the analysis of the second component of doublets (intervals of 3.5–19.5 msec) in Figure 2, the same method was used, but the bins were added together.

Blockers of glutamatergic receptors. For the experiments on evoked IPSCs using extracellular stimulation, 6-nitro-7-sulfamoyl-benzo[f]quinoxaline-2,3-dione (NBQX) (10 μM; Tocris Neuramin Limited, Bristol, UK) and D(−)-2-amino-5-phosphonopentanoic acid (APV) (50 μM; Tocris Neuramin Limited) were added to the bath to block excitatory synaptic transmission and to ensure that the observed IPSCs were evoked monosynaptically. NBQX and APV were omitted in the study of spontaneous IPSCs and in paired recordings; however, in these experiments EPSCs could readily be identified on the basis of their fast decay kinetics (Llano and Gerschenfeld, 1993) and were eliminated from the analysis.

RESULTS

Evidence for multivesicular release in recordings of spontaneous IPSCs

By analogy to the situation found at the neuromuscular junction, low receptor occupancy was implicitly assumed in the early formulation of the one-site, one-vesicle hypothesis (Triller and Korn, 1982). However, if one release event leads to a high degree of occupancy of postsynaptic receptors, the signal elicited by a second vesicular release would be reduced in amplitude, perhaps to the point of being undetected. Therefore, it is essential to know the degree of saturation of postsynaptic receptors after one release event to predict the effects of multivesicular release on

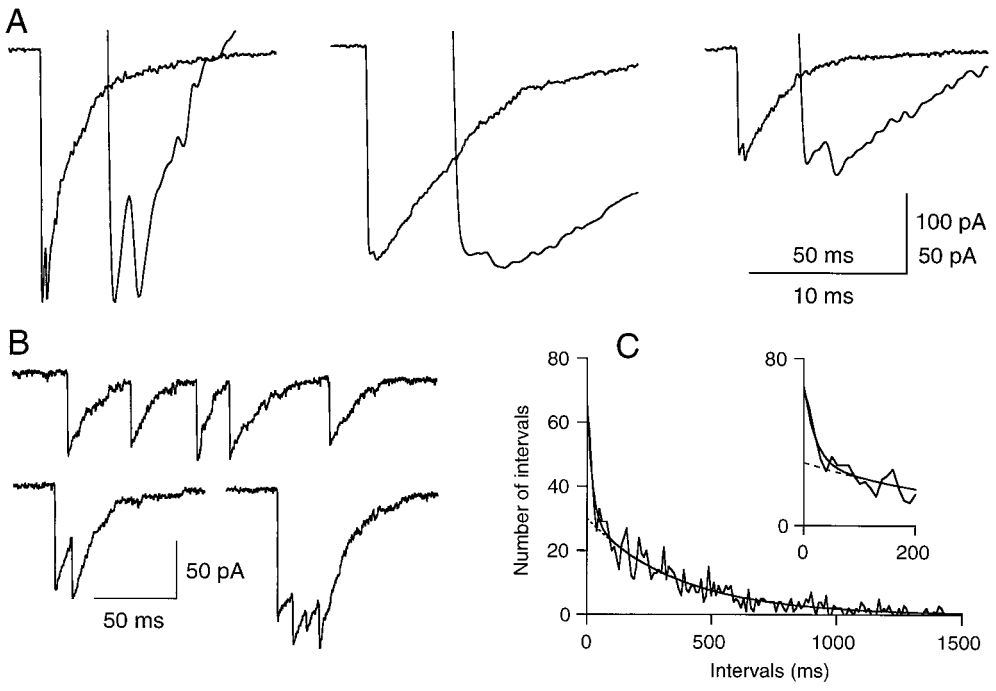

Figure 1. Multiple IPSCs in interneurons. *A*, Examples of closely spaced (<5 msec) IPSCs from an interneuron. Three double events are shown with two different time and amplitude scales to illustrate both the overall time course of the events and blow-ups of the peak region. Note differences in time course and amplitudes among pairs, and the match between peak amplitudes and time courses near the peaks within pairs. *B*, Further examples of repetitive IPSCs from the same recording. Here several events of similar amplitudes are separated by intervals of 5–50 msec. *C*, Distribution of intervals between successive events. The histogram (bin size: 10 msec; total duration of the recording: 7.5 min) is fitted with the sum of two exponentials with time constants of 20 and 357 msec. (A third, very fast component corresponding to double events such as illustrated in *A* is not displayed here.) Initial amplitudes for the fast and slow components are in a ratio of 1.2:1. *Insert*, Initial part of the interval distribution. The *dotted line* shows the slow exponential with a time constant of 357 msec.

synaptic transmission. An effective method for assessing the degree of saturation of postsynaptic receptors is to examine closely timed pairs of synaptic currents and to study in these pairs the relation between the amplitude of the second event and time interval (Tang et al., 1994). We have recently applied this approach to bursts of mIPSCs induced by applications of low concentrations of α-latrotoxin, and we concluded that the degree of occupancy of postsynaptic receptors after the release of a vesicle is high at interneuron–interneuron synapses (Auger and Marty, 1997; also see Nusser et al., 1997). If such is the case, multivesicular release would be revealed in IPSC recordings as closely successive events that do not summate linearly.

Correlations between consecutive IPSCs were examined in a series of six cells, where mean event frequencies ranged from 1 to 7 Hz. The number of events analyzed per cell ranged from 270 to 1191. Figures 1 and 2 illustrate the results for one of these cells. Inspection of the traces suggested that IPSCs were not independent of each other (Fig. 1). Many doublets were observed with short intervals (1–5 msec) between peaks. In most cases the peak amplitude of the second IPSC matched closely that of the preceding event. Furthermore, the IPSC profiles in the peak region were very similar for the first and second event of a pair, as illustrated for three different doublets in Figure 1*A*. The normalized slope of current decay (i.e., the slope divided by the peak current amplitude) was large for the first pair (0.276/msec for the first event and 0.237/msec for the second), low for the second pair (0.005/msec and 0.019/msec), and intermediate for the third pair (0.084/msec and 0.095/msec), and in each case the slopes were consistent within a pair. For longer time intervals (up to 50 msec), it was also clear that successive events were often coupled. In this time range bursts of events with homogeneous amplitudes were observed (Fig. 1*B*, *top trace*); nonlinear summation of the IPSCs indicating saturation of postsynaptic receptors was evident for time intervals below 20 msec (Fig. 1*B*, *bottom traces*). The distribution of interevent intervals could not be fitted with a single exponential, as would be expected from a Poisson process, but required three components. Two of these components are apparent in the plot of Figure 1*C*, and the third is illustrated in Figure 2*A*.

Three different mechanisms could explain a coupling between release events: (1) synchronous firing of presynaptic interneurons, (2) repetitive firing of interneurons at high frequency, and (3) delayed release of vesicles after one action potential. The first and strongest argument against synchronous firing of presynaptic interneurons is that it does not explain the finding that within a pair, the second IPSC is systematically smaller than the first. In addition, IPSC pairs are unlikely to result from synchronized excitatory inputs to different interneurons, because they can be demonstrated in the presence of blockers of ionotropic glutamate receptors, as exemplified by the results of Figure 6 below. An alternative source of synchronization could be electrical coupling, because an electron microscopy study reported the presence of gap junctions between interneuron dendrites in the molecular layer of rat cerebellum (Sotelo and Llinas, 1972). However, paired recordings in neighboring interneurons indicate a lack of firing synchronicity and a very low occurrence (2%) of electrical junctions (Vincent and Marty, 1996; Kondo and Marty, 1998). Altogether, the possibility of synchronous firing of presynaptic interneurons (mechanism 1) can be dismissed.

The distribution of interevent intervals in the range of 0–20 msec revealed two categories of doublets (Fig. 2*A*). There was first a large number of doublets in the first bin (intervals of 1.5–3.5 msec, corresponding to events such as those of Fig. 1*A*). In this bin, the number of pairs was 21, 3.6 times higher than predicted assuming superimposition of randomly occurring background IPSCs (*dotted line*). The probability of obtaining a number of double events of 21 or larger assuming a Poisson process given the mean IPSC frequency observed in this experiment can be calculated as 9×10^{-7} (see *Statistical test for event pairing* in Materials and Methods). Therefore, the amplitude of this first bin demonstrates a very significant degree of coupling for events at intervals of <3.5 msec. This was followed by a series of bins (intervals 3.5–19.5 msec; pairs corresponding to events such as those in Fig. 1*B*) where the frequency was consistently higher (by 1.2-to 2.1-fold)

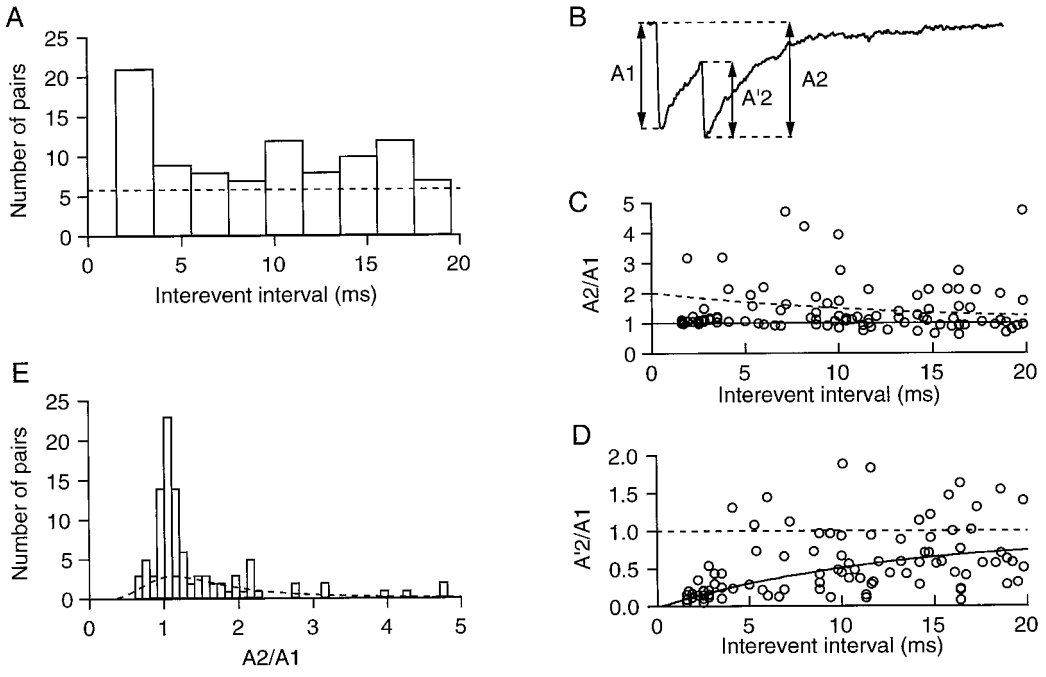

Figure 2. Analysis of event amplitudes in doublets. Same recording as illustrated in Figure 1. *A*, Histogram of occurrence of doublets for short interevent intervals. *Dotted line* indicates the number of doublets expected on the basis of random superimposition of background activity. *B*, Schematic diagram showing the current amplitudes measured for the analysis. A_1 and A_2 are measured from the baseline to the peak of the IPSC, A'_2 is measured from the onset to the peak of the IPSC. *C*, A_2/A_1 as a function of interevent interval. Most A_2/A_1 ratios are closer to the value of 1 predicted by total event occlusion after saturation of postsynaptic receptors (*continuous line*) than to the curve expected on the basis of the summation of independent events (*dotted line*; calculated from the mean decay kinetics of IPSCs). *D*, A'_2/A_1 versus interevent interval. The ratio $A^{2\prime}:A_1$ rises from a value that is close to 0 for short intervals up to ~1. Some of the points shown in *C* are off-scale in *D*. *Continuous line*: time course predicted for total saturation, calculated from the decay kinetics of IPSCs. Again, predictions made on the basis of independence (*dotted line*) fail to account for the data. *E*, Histogram of A'_2/A_1 ratios for the data shown in *B*. The *dotted line* represents predictions based on random superimposition of independent events (see Materials and Methods).

than that predicted on the basis of background activity. Again the probability that these numbers could be obtained on the basis of a Poisson process was very low ($p < 0.0002$). The maximum firing frequency of cerebellar interneurons is near 100 Hz at room temperature (Midtgaard, 1992; C. Pouzat, personal communication), indicating that the duration of their refractory period is on the order of 10 msec. Therefore, the early component (intervals of 1.5–3.5 msec) occurs during the refractory period of the presynaptic spike and corresponds to delayed release after one action potential (mechanism 3). On the other hand the excess events at 5–20 msec could be caused by either delayed release or repetitive presynaptic firing. Bursts of IPSCs were previously observed at interneuron–Purkinje cell synapses, indicating that interneurons occasionally fire at high rate (Vincent et al., 1992; Vincent and Marty, 1996). Multiple IPSCs with intervals in the 5–20 msec range often appeared as bursts with homogeneous amplitudes and regularly spaced time intervals (Fig. 1*B*), indicating that they were induced by repetitive firing of interneurons at high frequency (mechanism 2).

For intervals between 1 and 3 msec, the frequency of doublets was on average 5.0 ± 1.9 times higher (mean ± SEM; $n = 6$) than predicted on the basis of independence. In five out of six cells, the deviation from independence was significant at the $p < 0.02$ level. On average, however, the proportion of such doublets was rather small (range, 1.4–2.4%; $n = 5$; percentages corrected for background activity).

Mean ratios of doublet frequencies over values predicted on the basis of independence for intervals of 5–20 msec were 1.5 in the case of Figures 1 and 2, 1.7 in another cell, and close to 1 (range, 0.77–1.1) in the four other cases. Thus in four out of the six analyzed recordings, repetitive presynaptic firing was not sufficiently prevalent to give a detectable excess of doublets in this time window.

In summary, the results of Figures 1 and 2 show that spontaneous IPSCs in cerebellar interneurons are not randomly interspaced and that there is a significant pairing of events of similar sizes. In most experiments multiple release events occur at very short intervals, reflecting at least in part multivesicular release, whereas in some experiments, additional doublets with larger intervals reflect repetitive firing of the presynaptic cells.

Nonlinear summation of closely spaced spontaneous IPSCs

A quantitative analysis of spontaneous IPSC amplitudes for time intervals shorter than 20 msec is shown in Figure 2*B–E*. Amplitudes were labeled as illustrated in the diagram of Figure 2*B*. Baseline-to-peak (A_2) and onset-to-peak (A'_2) amplitudes of the second IPSC were divided by the baseline-to-peak amplitude of the first IPSC (A_1) to compare the two events in a doublet. Figure 2*C* shows that for most of the doublets with an interevent interval between 0 and 5 msec, the ratio A_2/A_1 is approximately 1. On the other hand, the ratio A'_2/A_1 (Fig. 2*D*) is very small for short intervals and increases for larger interval values. The distribution of A_2/A_1 ratios displays a broad component and a pronounced peak centered near 1 (Fig. 2*E*). A simulation of the distribution of A_2/A_1 ratios (see Materials and Methods) assuming linear

summation of randomly occurring IPSCs fitted both the shape and the amplitude of the broad component (Fig. 2*E*, *dotted line*). Therefore, the 0.9–1.2 peak of Figure 2*E* represents the extra events attributable to multivesicular release and repetitive presynaptic firing. Similar results were obtained in the other recordings. For intervals of 0–5 msec, the percentage of A_2/A_1 values between 0.8 and 1.2 was on average 73 ± 11% (mean ± SEM; n = 6). For comparison, the percentage predicted on the basis of independence from the amplitude distribution in the experiment illustrated in Figures 1 and 2 is 19%.

The nonlinear summation of closely spaced release events evident in Figure 2*D* is similar to that reported earlier for α-latrotoxin-induced IPSCs and could result from partial receptor saturation for events occurring at the same synaptic sites. Alternatively, the smaller second events could be caused by the liberation of a single vesicle at a site that has not released, whereas the first event would reflect the synchronized release of several vesicles at other release sites. If the second hypothesis was correct, the mean size of the second event in a pair should not depend strongly on the interevent interval and should be close to the mean amplitude of mIPSCs. Contrary to these predictions, the mean value of the second event amplitude, A'_2, clearly grew for intervals between 1 and 5 msec (Fig. 2*D*). Furthermore, the mean of A'_2 values at intervals of 1–3 msec (26 pA in the experiment illustrated) was markedly smaller than that of mIPSC amplitudes measured in tetrodotoxin (141 pA) (Llano and Gerschenfeld, 1993). This indicates that amplitude differences within doublets reflect at least partially receptor saturation after multiple release events at identical release sites, rather than asynchronous release at different sites.

A third explanation for amplitude occlusion could be that a first release event causes a local depolarization in the dendrite receiving the synaptic input and thus reduces the amplitude recorded for the second event, without necessarily implying receptor saturation. At the age investigated, interneuron dendrites have a simple morphology with a maximal length of ~50 μm and a diameter of ~1 μm (Llano et al., 1997), which is not expected to give rise to serious voltage escape associated with the sizes of synaptic signals recorded here. Nevertheless, the possibility of a nonlinear summation of IPSCs attributable to voltage-clamp errors was investigated. To this end, we measured evoked IPSCs as a function of membrane potential in control conditions and in the presence of 2 μM bicuculline, a dose that induced a reduction of the mean current amplitude to 20% of the control. Because voltage gradients in dendrites should be proportional to the current flow, voltage-clamp errors should be manifest as an alteration of the voltage dependence of the IPSC peak amplitude on addition of bicuculline. The ratio of the mean amplitudes at −30 mV to those at −60 mV was 0.526 ± 0.022 (n = 6) in control and 0.517 ± 0.017 (n = 4) in 2 μM bicuculline. Thus, halving the driving force resulted in a current reduction by nearly twofold, and the current ratio for the two potentials was the same in the control and in bicuculline. We conclude that voltage gradients in the dendrites cannot be the cause of the very strong reduction of the amplitude observed for short intervals.

Extracellular stimulation of a single presynaptic interneuron: some interneuron–interneuron connections involve a single release site

To pursue the mechanisms underlying double IPSCs, we next studied evoked IPSCs at individual interneuron–interneuron synapses. Postsynaptic currents were recorded in the whole-cell configuration, and a presynaptic interneuron was stimulated using a pipette filled with extracellular saline and positioned in the molecular layer. Once a connection was found, the synaptic responses to various stimulus intensities were recorded. If a single presynaptic neuron is stimulated, both the probability of obtaining a synaptic current and the mean amplitude of IPSCs (both excluding and including failures) should exhibit a clear threshold without further changes with increasing stimulus intensity (Raastad, 1995). Results were inspected visually during the experiments to judge whether these requirements were fulfilled, and if they were not, new presynaptic locations and, as needed, new postsynaptic cells were assayed. Confirmation that the response–intensity curve was stepwise was obtained later by off-line analysis (Fig. 3*A,B*). Some unitary synaptic connections showed a very simple amplitude distribution with two clearly separated groups of events: one group corresponding to the failures and the other corresponding to successful responses (Figs. 3*C*, 4). Simple amplitude distributions could generally be well fitted by a single Gaussian (Figs. 3*C*, 4; however see Fig. 7). Unless specified otherwise, only connections exhibiting simple distributions such as that of Figure 3*C* were used in the present study. These connections will be called hereafter "simple connections" or, for reasons that will be discussed below, "single-site connections."

At simple connections, the mean amplitude of evoked IPSCs (excluding failures) varied among experiments between 30 and 298 pA; the average across these means was 101 ± 74 pA (mean ± SD; n = 19; the corresponding CV value was 73%). This mean is similar to the average for mIPSC amplitudes (141 pA) (Llano and Gerschenfeld, 1993). The associated CV is also similar to that calculated from the variations among mIPSC amplitudes recorded in a given cell (e.g., 82% in the example in Auger and Marty, 1997, their Fig. 1). On the other hand, at individual simple connections, the CV of IPSCs excluding failures ranged from 10 to 31%, with an average of 19 ± 6% (mean ± SD; n = 19). These results indicate that although quantal sizes vary markedly among different simple connections, they are quite homogeneous for a given connection.

The probability of getting a response in simple connections was on average 28 ± 12% (mean ± SD; n = 19), varying between 10 and 54%.

Recent results at excitatory synapses indicate that amplitude distributions of miniature (Forti et al., 1997) and evoked synaptic currents (Gulyàs et al., 1993; Arancio et al., 1994; Silver et al., 1996) at single release sites are Gaussian. Therefore the shape of the amplitude distribution of Figure 3*C* suggests that the corresponding synapse involves only one release site. This proposal is consistent with the low success rate observed at simple synapses, because the probability of release at single release sites is usually assumed to be below 0.5 (Raastad et al., 1992). Further support in favor of the single-site hypothesis comes from a comparison between IPSCs recorded at simple synapses and bursts of mIPSCs resulting from application of low doses of α-latrotoxin (Auger and Marty, 1997). Like those observed at simple synapses, amplitude distributions for α-latrotoxin-induced bursts are Gaussian, with mean values that vary widely among bursts (range, 14–195 pA). Insofar as α-latrotoxin-induced bursts originate at single release sites (Auger and Marty, 1997), this similarity supports the view that the same applies for simple synapses.

Nevertheless alternative interpretations can be proposed. It is thus possible that several sites contribute to the response peak of simple connection amplitude histograms and that they cannot be distinguished because they have similar quantal sizes. In such a

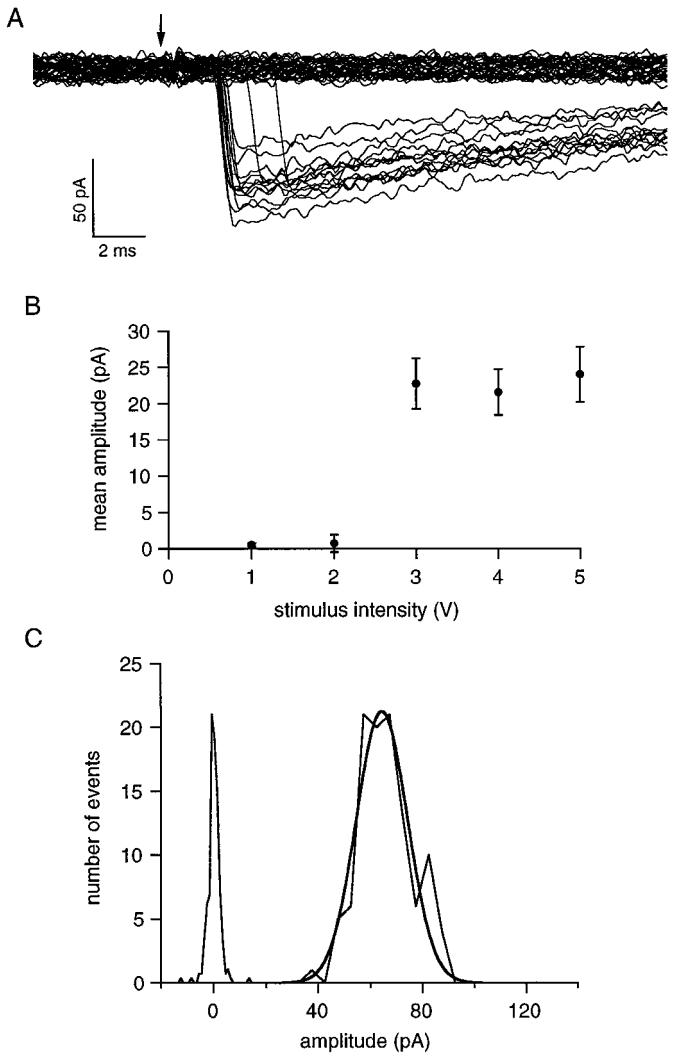

Figure 3. Single-site IPSCs elicited with external stimulation of a presynaptic interneuron. *A*, Fifty consecutive sweeps (except for 3 sweeps that were excluded because of contamination by background IPSCs) showing currents evoked by extracellular stimulation (5 V stimulus intensity). The time of the voltage step applied through the stimulation pipette is indicated by an *arrow*. Stimulation frequency is 1 Hz. An average failure sweep was subtracted from all displayed traces. Note that many stimulations result in transmission failures. *B*, Plot of mean amplitude (±SEM) versus stimulation intensity. The synaptic response has a sharp threshold for stimulations between 2 and 3 V, and there is no further increase with increasing intensity, indicating that there is no further recruitment of presynaptic connections. Such a stepwise dose–response curve is one requirement to ensure that a single presynaptic neuron is stimulated. *C*, Amplitude distributions for stimulations that elicited postsynaptic responses (bin size 10 pA) and for the failures (bin size 1 pA) (stimulus intensity: 5 V). The failures distribution was scaled to the distribution of IPSCs to allow comparison of the SDs. A Gaussian fit of the responses distribution is superimposed (*thick line*). $n = 350$ stimulation trials. The probability of successful responses was 32%; mean amplitude, 66 pA; CV (corrected for background variance), 13%. This type of distribution most likely corresponds to a single release site.

case, simultaneous release from two of these sites should generate a secondary peak with twice the amplitude of the first. For example, if one assumes two independent sites with equal release probabilities, the amplitude of the secondary peak is expected to be 10.6% of that of the first in the case of Figure 3*C*; no evidence for such a component is apparent. Similar arguments can be made for more than two release sites or for release sites with different release probabilities. Therefore it is unlikely that several independent release sites generate the histogram of Figure 3*C*.

Next, the possibility of several coupled release sites was considered. At some mossy fiber–granule cell synapses, EPSC amplitude histograms display a single peak with low variance attributable to the simultaneous activation of several release sites (Silver et al., 1996). Such a configuration is unlikely in the present case because of the high failure rate. However, it could be considered as a possible model for simple synapses if most failures were caused by stimulation or propagation failures, whereas responses would correspond to the simultaneous activation of several sites having a very high release probability. In granule cell synapses, the existence of multiple release sites was revealed by lowering the external Ca^{2+} concentration, which induced a reduction of the mean amplitude of responses, excluding failures (Silver et al., 1996). As will be documented next, very different results were obtained in interneuron–interneuron synapses, such that the hypothesis of several coupled release sites could be dismissed.

Lowering the probability of release at simple synapses

The probability of release was reduced by lowering the external Ca^{2+} concentration to see how this would affect the amplitude histograms of the responses. Lowering the external Ca^{2+} concentration to 1 mM or less often led to very low response probabilities that could not be analyzed quantitatively. The Ca^{2+} concentration was therefore usually lowered to 1.5 mM. The external Mg^{2+} concentration was increased to maintain the total concentration of divalent ions constant and to limit modifications of surface potential attributable to ionic changes.

Figure 4*A* shows the effect of lowering the external Ca^{2+} concentration from 2 to 1.5 mM on the distribution of a simple connection. The probability of release is reduced by 50%, from 34 to 17%. The mean amplitude of the responses (excluding failures) is minimally affected, with a slight decrease from 131 to 120 pA. Quite importantly, there is no fragmentation of the initial peak into several smaller amplitude components. Rather, consecutive events have more homogeneous amplitudes in the low Ca^{2+} period than during controls (Fig. 4*A,B*). This translated into a strong and reversible reduction of the CV from 19.7 to 9.2% (Fig. 4*C*).

In contrast to the results illustrated in Figures 3 and 4, amplitude distributions at "complex" unitary connections are broad and skewed, presumably corresponding to multisite connections. In the example of Figure 5, the mean response amplitude (excluding failures) decreased from 283 to 226 pA after the external Ca^{2+} concentration was lowered to 1.5 mM, whereas the CV increased from 53 to 64%. The mean amplitude was further reduced (to 165 pA) after the Ca^{2+} concentration was lowered to 1 mM.

On average, reducing the external Ca^{2+} concentration from 2 to 1.5 mM (increasing the Mg^{2+} concentration from 1 to 1.5 mM) at simple connections decreased the probability of responses to 65 ± 18% of the control value (mean ± SD; $n = 5$). In 1.5 mM Ca^{2+}, the average amplitude of the responses (excluding failures) and the CV decreased to 90 ± 6 and 72 ± 18%, respectively, of the control (mean ± SD; $n = 5$). Both decreases were statistically significant ($p < 0.05$). If the responses were coming from several release sites with a very high probability of release, lowering the probability of responses should sometimes desynchronize them, and smaller amplitude responses should be observed, causing a dramatic increase in CV. There was no evidence for such a fragmentation of the initial peak, confirming that the responses come from a single release site.

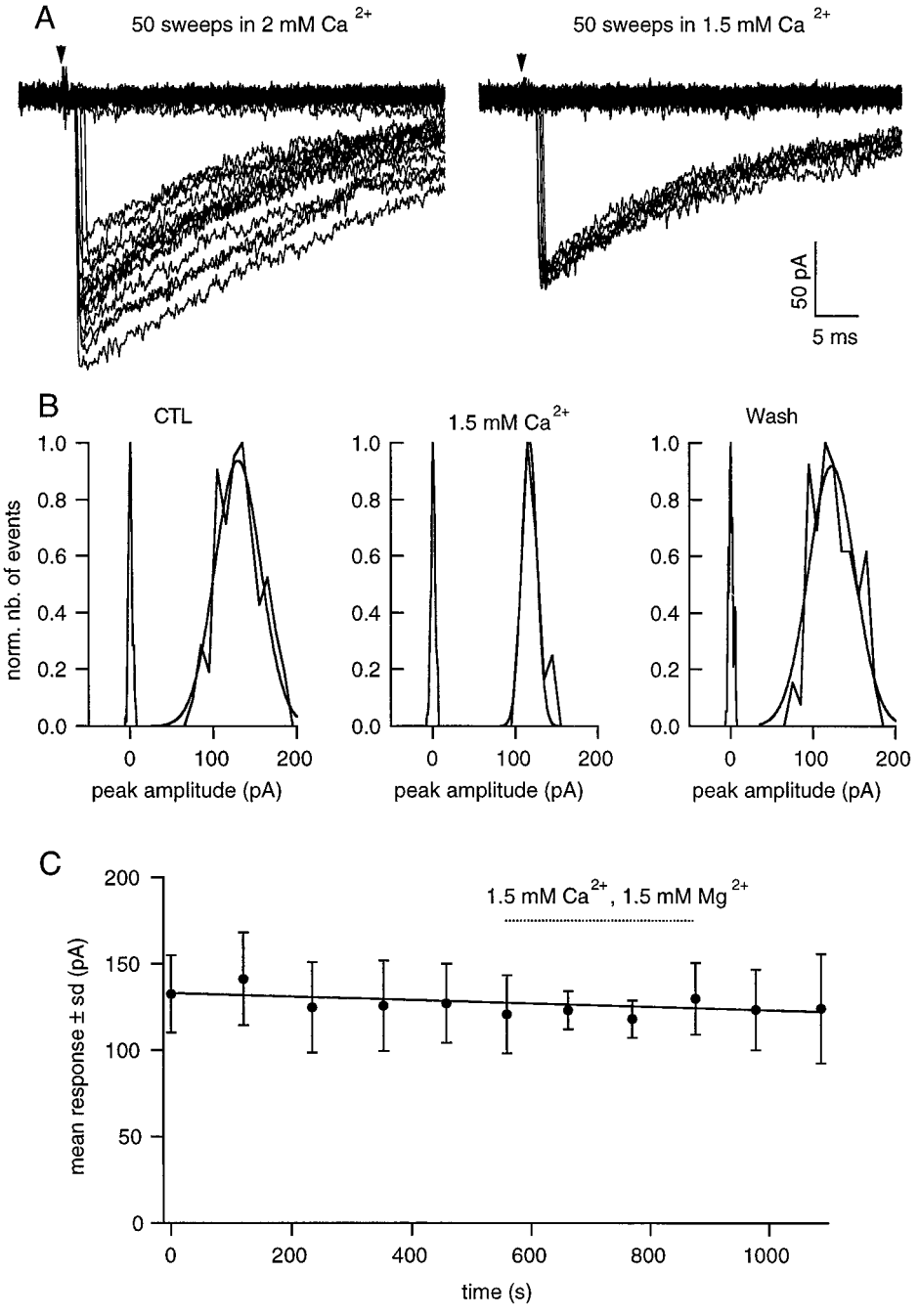

Figure 4. Effect of lowering the external calcium concentration at a single-site connection. *A*, Fifty consecutive sweeps in the presence of 2 mM Ca^{2+} and 1 mM Mg^{2+} (*left*), and 1.5 mM Ca^{2+} and 1.5 mM Mg^{2+} (*right*). Successful responses are less frequent and have more homogeneous amplitudes in the low Ca^{2+} solution. *Arrowheads* indicate stimulation timing. An average failure sweep was subtracted for display. *B*, Amplitude distributions. *Left*, *CTL*, 2 mM Ca^{2+} and 1 mM Mg^{2+}. $n = 500$; proportion of failures: 65.8%; mean amplitude of responses (excluding failures): 131 ± 26 pA; CV = 19.7%. *Middle*, 1.5 mM Ca^{2+} and 1.5 mM Mg^{2+}. $n = 200$; proportion of failures: 83%; mean of responses: 120 ± 11 pA; CV = 9.2%. *Right*, *Wash*, $n = 200$; proportion of failures: 58.7%; mean of responses: 122 ± 24 pA; CV = 19.7%. *C*, Mean amplitude of responses (excluding failures; each point corresponds to 100 stimulation trials) versus time. The line is a linear fit of the control data; its negative slope reflects a slow rundown of the responses. In the presence of 1.5 mM Ca^{2+}, the amplitude decreases slightly below the regression line, and the SD decreases by ~50%. Both effects are reversible.

Changing the external Ca^{2+} concentration alters the excitability of neurons such that a diminution of Ca^{2+} is expected to increase the rate of firing of presynaptic cells (Frankenhaeuser and Hodgkin, 1957). Although the effect on firing threshold would run counter to the observed increase of the failure probability, it seemed desirable to reduce the release probability at single-site synapses without altering the external Ca^{2+} concentration. Preliminary tests indicated that 5 μM Cd^{2+} blocks ~50% of the Ca^{2+} currents recorded in the soma of interneurons ($n = 3$; data not shown). Because the probability of responses is already very low in control conditions at single release site synapses, it was decided to reduce the release probability by adding only 2.5 μM Cd^{2+} to the external medium. On average, the probability of responses was decreased to 60 ± 25% of the control (mean ± SD, $n = 7$). The block was variable from connection to connection, varying from 4 to 74%. On average, the mean response amplitude and CV were little affected by the addition of Cd^{2+}; they were 93 ± 15 and 96 ± 29%, respectively, of the control ($n = 7$). Neither of these slight reductions was statistically significant. Again, no fragmentation of the amplitude distribution was observed, indicating that the responses do not result from synchronized release of vesicles at several release sites but come from a single functional release site. In some cases, the CV was significantly reduced, but this was not observed as regularly as when the external Ca^{2+} concentration was lowered.

Altogether these results exclude the possibility that simple synapses involve several release sites with high release probabil-

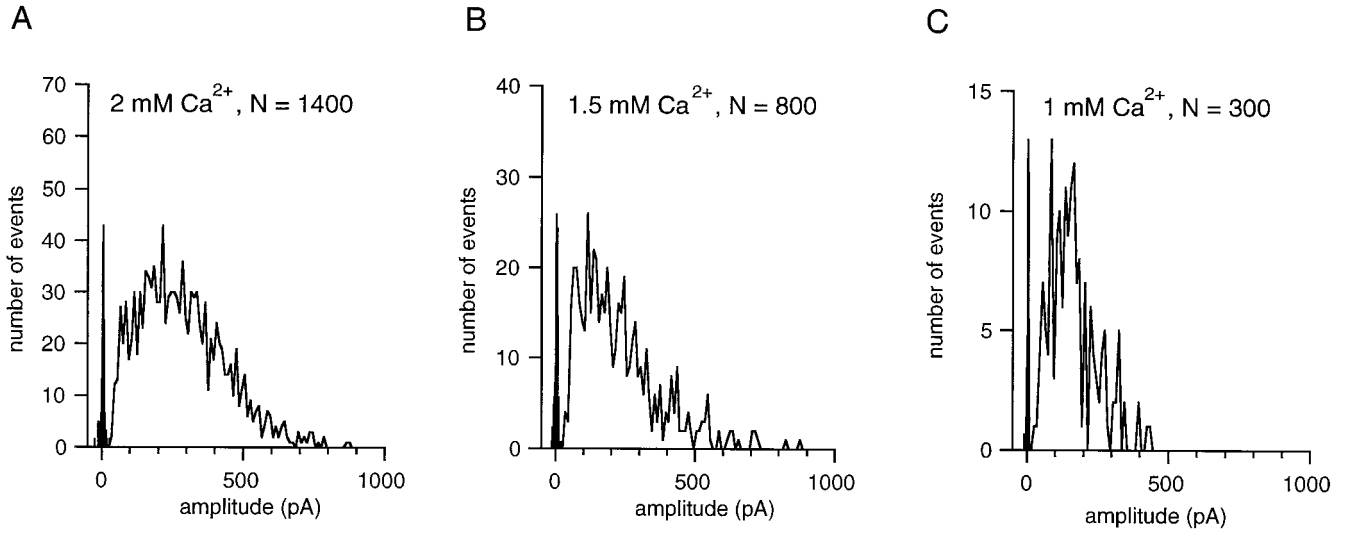

Figure 5. Effect of lowering the external Ca^{2+} concentration at a multisite connection. *A*, Control amplitude distribution. $n = 1400$; probability of failures: 17%; mean amplitude: 283 ± 151 pA; CV = 53.4%. *B*, Distribution in the presence of 1.5 mM Ca^{2+}, 1.5 mM Mg^{2+}. $n = 800$; probability of failures: 35%; mean amplitude: 226 ± 146 pA; CV = 64.4%. Note that for a decrease of release probability of only 25%, the distribution is shifted to the left, the mean amplitude decreases by 20%, and the CV increases by 20%. *C*, Distribution in the presence of 1 mM Ca^{2+}, 2 mM Mg^{2+}. $n = 300$; probability of failures: 44%; mean amplitude: 165 ± 83 pA; CV = 50.4%.

ities. Therefore we conclude that such connections involve single functional release sites.

An explanation for the reduction in amplitude and CV observed in some experiments (particularly when reducing the extracellular Ca^{2+} concentration) is suggested by the above conclusion that several vesicles can be released at a single site. In such a case, decreasing the probability of release should result in a decrease of the mean number of vesicles contributing to each IPSC. This should result in a reduced amplitude. As the proportion of multivesicular IPSCs is reduced, the proportion of events involving single vesicular release is expected to increase. Thus one component of the variance of the IPSC amplitudes is gradually suppressed, and this could account for the decrease in CV observed in some cases. However, the expected effects on mean amplitude and CV are modest if the occupancy of the postsynaptic receptors is high. In addition, the extent of these effects depends on the mean occupancy of the receptors and mean number of released vesicles per spike in control conditions. Because such parameters are likely to be specific for each release site (Auger and Marty, 1997), results are expected to vary widely from one experiment to the next.

Multivesicular IPSCs at single-site interneuron–interneuron synapses

We next examined whether multiple events similar to those obtained in spontaneous IPSC recordings could be detected in evoked IPSCs obtained at single-site connections. A typical recording is illustrated in Figure 6. The analysis reveals a number of doublets for intervals up to 20 msec (Fig. 6*Aa,B*). Only clear-cut doublets, for which two peak amplitudes could be measured unambiguously (Fig. 6*Aa*), were considered for the plots of Figure 6*B–D*. Additional traces suggested the occurrence of multiple events, which however could not be unambiguously resolved (Fig. 6*Ab*). In the 0.5–1.5 msec bin, the number of doublets is 92 times higher than that expected from the level of background synaptic activity (Fig. 6*B*, *dotted line*), so that contamination of the results by signals coming from other synapses could be neglected. A clear excess of doublets occurs for intervals up to 5 msec. In this interval range, most of the doublets display an A_2/A_1 ratio between 1 and 1.5, indicating event occlusion and high occupancy of the postsynaptic receptors (Fig. 6*B–D*).

Extracellular stimulation experiments can lead to the uncontrolled release of neurotransmitters and damage of surrounding cells (Hamann and Attwell, 1996). Although it is unclear how such changes could have produced results such as those of Figure 6, it seemed important to show that the same results could be obtained without resorting to extracellular stimulation. We have recently described paired recordings of connected presynaptic and postsynaptic interneurons (Kondo and Marty, 1998). On the basis of IPSC amplitude distributions, it was found that ~50% of the interneuron–interneuron connections are multisite, and that the other half has primarily one site, which is contaminated by slow currents of unknown origin in ~25% of the cases and is free from such contamination in the remaining 25%. Multivesicular IPSCs were clearly apparent in the last category of paired recordings, thus showing that the results in Figure 6 are not an artifact of extracellular stimulation. Of a total of seven single-site synapses that were examined (three with paired recordings and four with extracellular stimulation), six showed results similar to those of Figure 6, with a significant ($p < 0.02$) excess of doublets for intervals <3 msec over the number expected from the background rate of spontaneous IPSCs. The mean value of the A_2/A_1 ratio varied among these experiments between 1.17 and 1.45, with an overall mean of 1.30. By using Equation 3 in Appendix 1, it is possible to calculate the occupancy of postsynaptic receptors from this ratio. The result, 0.70, is close to the mean value of 0.76 derived from the analysis of α-latrotoxin-induced bursts (Auger and Marty, 1997). In these experiments the percentage of resolvable doublets, with an estimated time resolution of 0.5 msec (see Materials and Methods), varied between 3 and 6% of the successful responses and had a mean of 4.3%.

The lack of linear summation of the IPSCs in doublets indicates that they activate the same set of receptors and come from the same release site. Overall the results indicate that more than

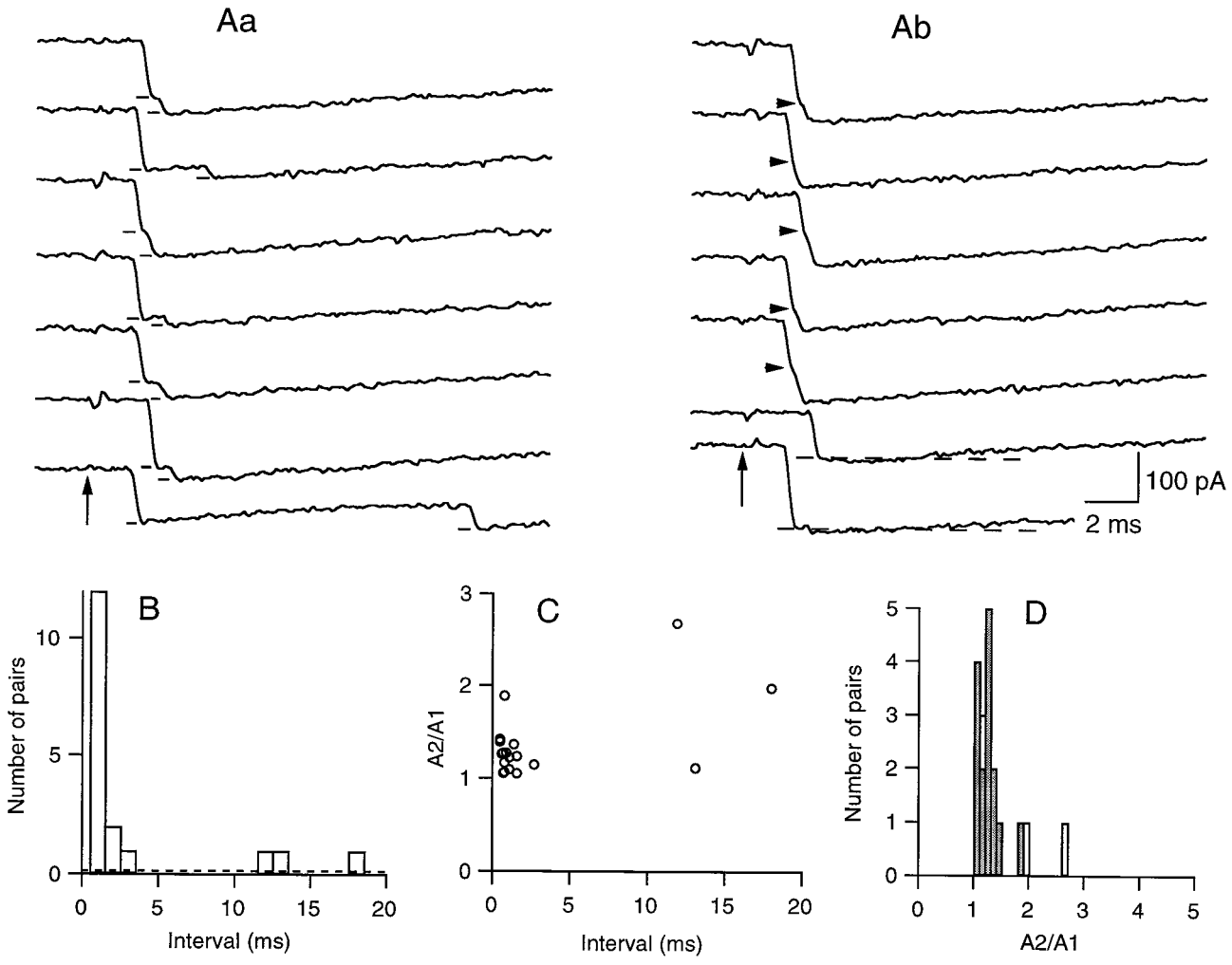

Figure 6. Analysis of doublets for a single-site synapse. Data from a single-site connection (same experiment as in Fig. 4; results with control external solution) were analyzed as in Figure 2. *Aa*, Some IPSCs are followed by a secondary event. Measured values of A_1 and A_2 are indicated by *short horizontal lines*. *Ab*, Many events display an inflection point (*arrowheads*) in their rising phase. The two lower traces in *Ab* illustrate traces with a shallow minimum occurring 1–2 msec after the main current transition, indicating unresolved late vesicular release. All traces in *A* are taken from a sequence of 111 sweeps, during which a total of 51 responses were recorded. Of these, seven contained the doublets shown in *Aa*, and eight contained unresolved multiple events as shown in *Ab*. The timing of extracellular stimulations is indicated by *arrows*. *B*, The frequency of doublets decreases abruptly with intervals up to 5 msec. *Dotted line*, Frequency of doublets expected from random superimposition of evoked IPSCs with background IPSCs. *C*, A_2/A_1 ratios are mainly between 1 and 1.5, particularly for intervals shorter than 5 msec. *D*, Histograms of A_2/A_1 ratios, both for the entire interval range (0–20 msec, *open bars*) and for intervals <5 msec (*shaded bars*).

one vesicle can be released at a single site in response to a single action potential.

Resolution of monovesicular and multivesicular events in certain single-site recordings

"Simple" or "single-site" synapses have been defined as synapses where amplitudes of successful IPSCs were grouped in a single component. In some of these recordings it was possible to further distinguish two closely spaced amplitude levels. One example is shown in Figure 7*A*. The amplitude histogram from these data were better fitted with a double Gaussian than with a single one (Fig. 7*B*) (maximum likelihood ratio test; $p \ll 0.001$). To test whether the two levels could have resulted from a drift in the mean amplitude of IPSCs, the recording was split into two ranges of equal duration. The bimodal appearance of the amplitude histogram and the positions of the amplitude levels were conserved in the two consecutive data periods (Fig. 7*C*), arguing against a drift in the quantal size. Further support for the existence of two classes of events was given by the observation of double events jumping from one level to the other (in which case the only value that was entered in the amplitude histogram was the higher one), as well as of inflection points in the rise phase of the larger events near the peak amplitude of the smaller component (Fig. 7*A*).

Could the distribution of Figure 7*B* be generated by two independent sites? If the amplitudes of the two sites were to correspond to the positions of the two peaks, one would expect to see an additional peak with an amplitude corresponding to the sum of the two components. If we now assume that the larger peak results from the simultaneous activation of events from the first peak and of events generated at another site, we would expect to obtain a component at an amplitude equal to the difference between those of the two peaks. Because additional components corresponding to the sum or to the difference of the amplitudes of the two peaks are absent, it appears that the two levels are not

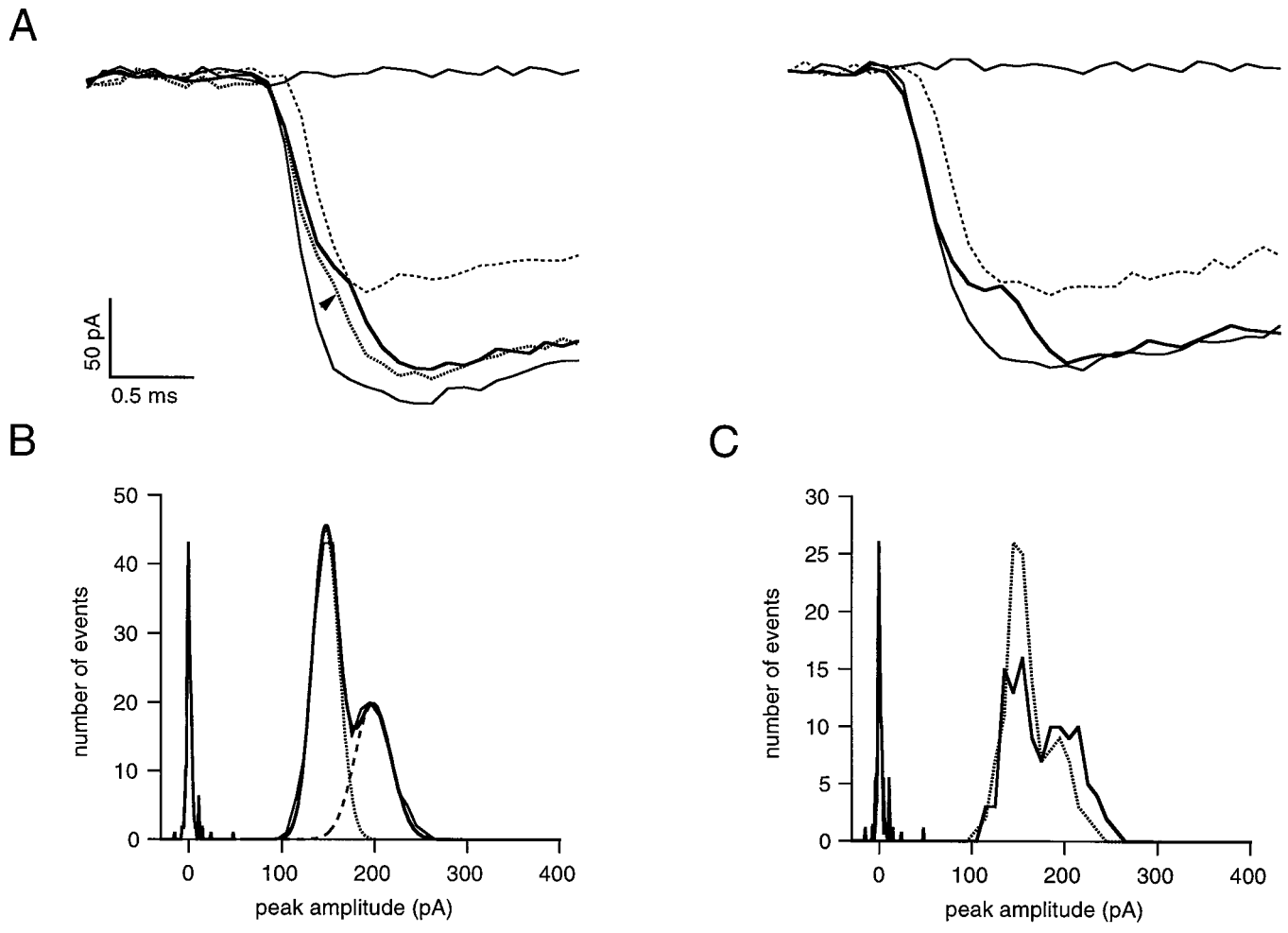

Figure 7. A single-site synapse with two closely separated amplitude components. *A*, In this single-site recording, two distinct amplitude levels were observed. In several traces, double events were seen to jump from one level to the other (*thick line* responses), or to display an inflection point near the lower amplitude level (*arrowhead*). *B*, Overall amplitude histogram from this experiment (480 trials), showing two distinct peaks. In dual component traces only the peak amplitude of the second event was entered. The histogram was fitted to the sum of two Gaussian curves (*thick line*; *dotted lines* indicate each curve separately) with mean amplitudes and SD values of 147 ± 14 pA and 198 ± 20 pA, respectively. The scaled noise histogram is also shown (failure rate was 0.50). *C*, Histograms for first (*thick line*) and second (*dotted line*) halves of the data. Although the proportion of events in the higher amplitude peak decreased from the first to the second data range, the two peaks appear in both cases.

generated by two independent sites. Thus, the events of the two peaks interact strongly with each other. For example, if the larger amplitude events result from the summation of events coming from the first site and from smaller events originating at a second site, all failures at the first site need to induce failures at the second site, implying that all failures at the first site are stimulation or propagation failures, which is an unlikely hypothesis. Thus, the simplest interpretation of the results is that all events originate at a single release site, that lower amplitude events represent single vesicular release, and that the larger ones represent multivesicular events.

The two-component Gaussian analysis of Figure 7*B* indicates that the low and high amplitude components are centered at 147 and 198 pA, respectively. The ratio between these two values is $A_2/A_1 = 1.34$, similar to the mean ratio found from the doublet analysis illustrated in Figure 6. It is again possible to estimate the occupancy of postsynaptic receptors, ω, by using Equation 3 in Appendix 1. The result is $\omega = 0.66$. In two other similar cases the calculated occupancy values were 0.53 and 0.48. Overall the values of ω are somewhat lower than those calculated on the basis of double event analysis (0.48–0.66 vs 0.55–0.83). Two factors should contribute to give low ω values with the present method. First, the large amplitude peak is likely to contain multiple release events together with two-release events, leading to an overestimate of the A_2/A_1 ratio. Second, the identification of the two levels is easier for synapses with unusually high A_2/A_1 ratios, and therefore the method of Figure 7 presumably selects experiments with low occupancy values.

From the integrals of the two Gaussians in Figure 7 it was calculated that 61% of the responses corresponded to single release events and 39% to multiple (probably mostly double) events. Thus the mean number of released vesicles per successful response is at least $2 \times 0.39 + 1 \times 0.61 = 1.39$. The corresponding values for the two other experiments were 1.38 and 1.13.

The decay of GABA currents after short applications of GABA to outside-out patches is independent of the GABA concentration (Jones and Westbrook, 1995; Galarreta and Hestrin, 1997). Therefore, if two vesicles are released simultaneously, the resulting current is expected to decay like a single-vesicle IPSC, but if there is jitter among release events, postsynaptic receptors should

be exposed to a longer effective GABA pulse for a two-vesicle release, and they should respond with a slower rise time as well as with a slower decay (Jones and Westbrook, 1995). To test these predictions, the kinetic properties of the presumed single- and double-vesicle components were compared. Traces from each class of events were selected on amplitude criteria by using the two-Gaussian analysis of Figure 7*B*. In each category, individual traces were aligned with respect to the time point corresponding to 25% of the maximum amplitude, and they were then averaged together. As predicted, the average decay time course of the larger events was slower than that of the smaller ones (Fig. 8*A*), although the average rising phase was slower and the peak was more rounded (Fig. 8*B*). Similar effects were found in the two other cases of double-peaked single-site histograms. In outside-out patches, increasing the duration of a GABA pulse leads to a slower decay of the current attributable to an increase in the weight of the slow component, whereas neither the fast nor slow component time constants are modified (Jones and Westbrook, 1995). In interneurons, decay kinetics differs among release sites (Auger and Marty, 1997). Of the three cases observed, only the connection presented in Figures 7 and 8 had a biexponential IPSC decay. In this case, as predicted from the above data, the time constants for the fast and slow components were not modified, and the weight of the slow component was increased for the large events (Fig. 8). Altogether the results suggest that the larger events result from the summation of slightly desynchronized release events.

Correlation between amplitudes and latencies at single-site synapses

The results of Figures 7 and 8 suggest that multivesicular events occur frequently, but that they are difficult to resolve because of a high degree of synchrony among release events. In such a situation, multivesicular release at single-site synapses may impose a link between first latency and peak amplitude of IPSCs. If several events occur in close succession, a large amplitude is obtained because of sublinear summation of individual events. In such a case it is the latency of the first event that is measured, because the analysis program selects the time point of the first clear deviation from baseline to calculate the latency. Thus unresolved multivesicular events are registered as single IPSCs with, on average, large amplitudes and short latencies. Conversely, late latencies tend to be associated with single release events, and therefore with small peak amplitudes, because the probability that a late release would be followed by another one is low. In agreement with these predictions, we found in extracellular stimulation experiments at simple synapses that peak amplitudes are negatively correlated with first latencies (Fig. 8*C*).

It is conceivable that latency measurements obtained using extracellular stimulation could be distorted by the unknown delay between stimulation and presynaptic firing. Therefore we also performed latency analysis on data obtained in paired recordings (Fig. 9). Figure 9*A* illustrates an example from a simple synapse. Latency distributions had a single peak occurring 1–1.5 msec after the peak of the presynaptic spike, and they trailed up to 2–3 msec after the presynaptic spike. When all data points were considered, a significant correlation was found between latency and amplitude ($p < 0.01$). A regression line through all data points had a slope of −22 pA/msec. Figure 9*B* illustrates the results from the experiment that gave the strongest correlation from a complex connection. In this case the slope was much larger (−502 pA/msec), and the correlation was highly significant ($p < 0.001$). Overall 17 pairs out of 20 showed a statistically significant negative correlation between the two factors ($p < 0.05$), and no significant positive correlation was found. The strength of the correlation was larger for multisite connections than for single-site connections. This is illustrated in Figure 9*C* where normalized slopes (i.e., slopes divided by the mean current amplitude) are displayed for single-site connections (*left panel*; $n = 9$) as well as for multisite connections (i.e., for the rest of the paired recordings) (*right panel*; $n = 11$). The stronger slope obtained at multi-

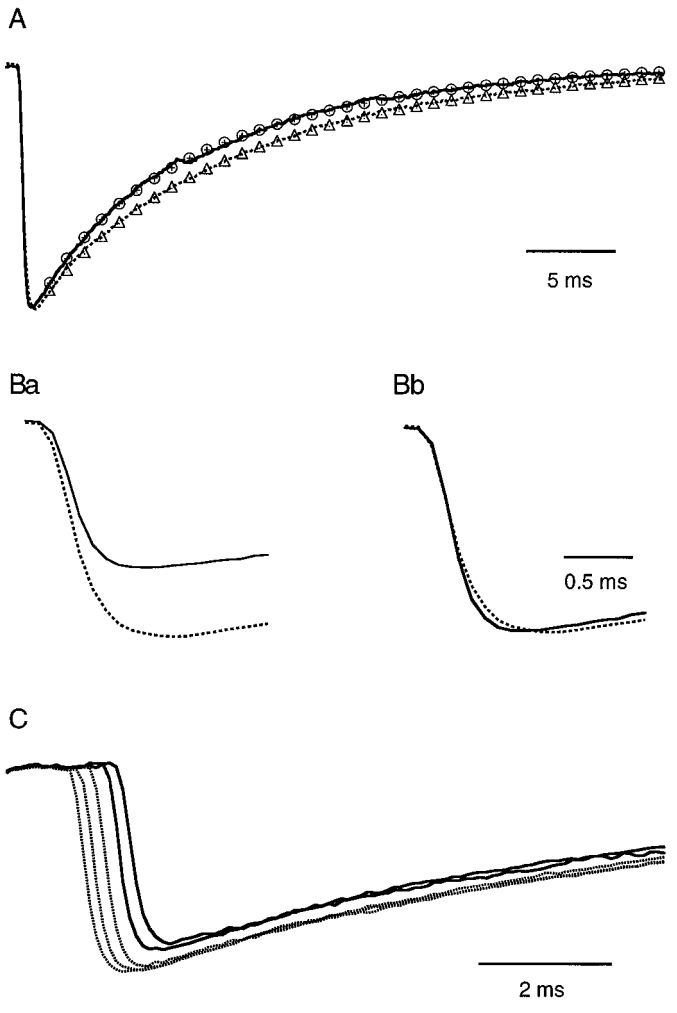

Figure 8. Kinetics of single and multiple events. Same data as in Figure 7. In *A* and *B*, the data have been split into two components: a low amplitude component, up to 150 pA, and a high amplitude component, for amplitudes larger than 180 pA. These threshold values were chosen such that each component contains almost exclusively events from one or the other of the two Gaussians used to fit the histogram in Figure 7*B*. *A*, Superimposed normalized means of the low (*continuous line*) and high (*dotted line*) amplitude components. Rising phases of individual events were aligned before averaging. The decay phases of the high and low amplitude IPSCs have been fitted using double-exponential curves, with respective parameters: $\tau_{fast} = 2.6$ msec, $\tau_{slow} = 12.9$ msec; weight of the slow component: 91% (high amplitude); $\tau_{fast} = 3.4$ msec, $\tau_{slow} = 12.1$ msec; weight of the slow component: 78% (low amplitude). *B*, Rising phases of the mean two components without scaling (*a*) and after normalization (*b*). The high amplitude component has a more prolonged rise time (+0.2 msec) and a more rounded peak. *C*, Mean currents grouped according to latency. The latencies range from 1.1 to 2.1 msec after the end of the stimulation artifact in 0.2 msec increments. The earlier latency values correspond to larger currents (*dotted lines*), whereas the later latencies correspond to smaller current amplitudes (*continuous lines*).

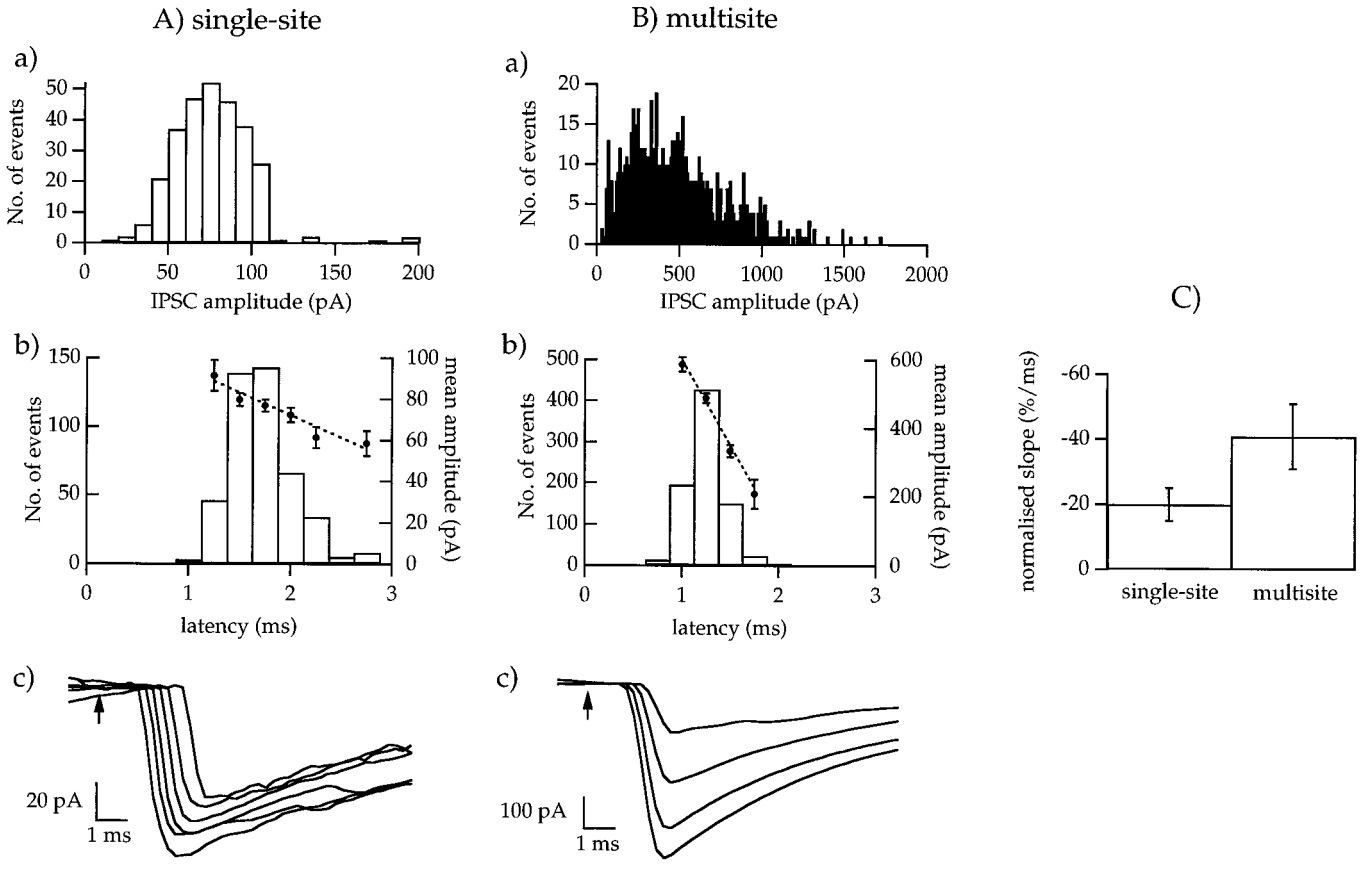

Figure 9. Latency–amplitude correlation in paired recordings. Results in *A* and *B* are from a single-site and multisite synapse, respectively. *a*, Amplitude histograms (failures are not shown). *Aa*, Mean current amplitude, 75 pA; total number of trials, 774; failure rate, 0.63. *Ba*, Mean current amplitude, 476 pA; total number of trials, 868; failure rate, 0.06. *b*, Latency distributions. Latencies are measured from the peak of the presynaptic action potential-related signal measured in the cell-attached mode. For each latency bin that contained more than five events, mean amplitude values ± SEM are displayed. Amplitudes are significantly correlated to latencies ($p < 0.01$). Regression lines have been drawn to the data, with slopes of −22 pA/msec (*A*) and −502 pA/msec (*B*). *c*, Average traces for latency bins in *b* containing more than five events. *C*, Summary data for 9 single-site synapses and 11 multisite connections. Some of the single-site synapses were contaminated with "slow" synaptic currents (Kondo and Marty, 1998). *Aa* is reproduced from Kondo and Marty, 1998.

site connections is easily explained, because at these synapses many release events arise at different sites, in which case their amplitudes add together, whereas at single-site synapses receptor saturation results in sublinear amplitude summation.

We have modeled the amplitude–latency correlation at single-site synapses by assuming a common time-dependent release probability function for all vesicles available for release (Appendix 2). Figure 10 shows simulations modeling the data illustrated in Figure 9*A*. A first simulation assumed a time-dependent release probability function that was the same for all trials. The resulting curves strongly deviated from the data for all tested values of ω ($\geq$0.5) (Fig. 10*A*). Because other results (Auger and Marty, 1997; Nusser et al., 1997; and present work) indicate values of ω in excess of 0.6, we conclude that the underlying model is inadequate. To obtain enough variation of the mean amplitude with latency, it was necessary to increase the mean number of vesicles simultaneously released per trial. We then assumed that the probability of vesicular release is not constant from one trial to the next and that for some trials this probability was 0 at all times, whereas for the other trials it had the reproducible time profile $p(k)$. With these assumptions the failure rate for effective trials (those for which $p > 0$), F', is lower than the measured failure rate F. Equations 7–17 are nevertheless valid provided that F is replaced by F'. Thus m', the mean number of vesicles per effective trial, is $-ln\ F'$, not $-ln\ F$ (see Eq. 2). By assuming a value of 2 for m' (instead of $m = 0.462$ in panel *A*), a good fit was obtained with occupancy values between 0.6 and 0.7 (Fig. 10*B*). The value $m' = 1$ gave a good fit only for $\omega \sim 0.5$, which was considered too low. The value $m' = 4$ gave a shallow variation of the mean amplitude with latency for the first millisecond, attributable to receptor saturation, which did not match the experimental data. Therefore the value $m' = 2$, although approximate, can be regarded as a realistic estimate for this experiment, within the framework of the model exposed in Appendix 1 and 2. $m' = 2$ corresponds to a mean vesicle number of 2.31 per successful response.

As can be seen from Figure 10, the maximum slope of the amplitude–latency plot increases with m' and decreases with ω. Because m' is different in Figure 10*Ac,Bc*, it can be seen that for the same occupancy the slope of the amplitude–latency relation is different. A slope of 20%/msec, corresponding to the mean value for single-site synapses in Figure 9*C*, is obtained for $\omega = 0.6$ and $m' = 0.6$. Because our estimate of ω is larger than 0.6, we infer that m' is on average larger than 0.6. According to the Poisson statistics exposed in Appendix 1, this corresponds to a mean

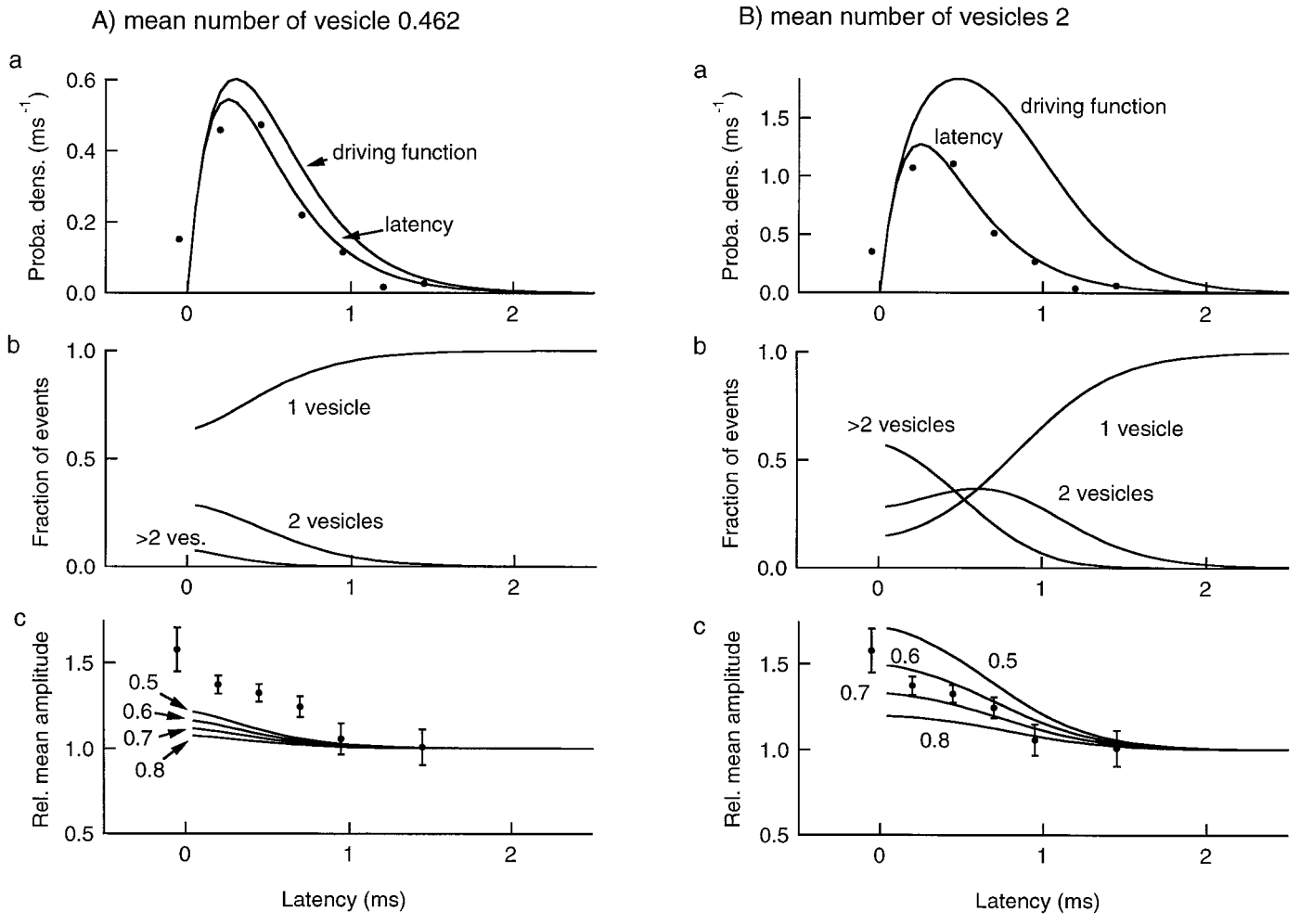

Figure 10. Simulation of latency–amplitude correlation. Data from the experiment illustrated in Figure 9*A*. Simulations were made for a single-site synapse assuming various degrees of multivesicular release and receptor saturation. *A*, In this section the mean number of vesicles released per trial is 0.462, as calculated from the failure frequency for a pure Poisson process. The *top panel* (*a*) shows the original latency data (*dots*; bins of 0.25 msec), a corresponding model latency distribution, and the associated "driving function" describing the probability density of synaptic vesicles to undergo exocytosis (Eq. 8; $\tau = 0.25$ msec; see Appendix 2 for details). Latencies are shifted by 1.3 msec so that 0 time is the origin of the driving function. The *middle panel* (*b*) shows the calculated proportions of events corresponding to the fusion of one, two, or more than two vesicles as a function of latency. Note that the fraction of events with multivesicular release drops very quickly with time. The *bottom panel* (*c*) shows simulations of the mean amplitudes as a function of latency, assuming occupancy values of 0.5, 0.6, 0.7, and 0.8. None of these simulations comes close to the experimental data (*dots*; error bars show ± SEM). *B*, For these simulations the density probability of vesicular release was allowed to fluctuate between 0 for some of the trials and a constant driving function in the other trials. This introduced one more free parameter than in the simulations shown in *A*. For the simulation shown here the mean number of vesicles that was chosen was two. *a*, *b*, and *c* are arranged as in *A*. Occupancy values between 0.6 and 0.7 give a good fit to the data.

vesicle number of >1.33 per successful response and to a proportion of multiple events of >27% among successful responses.

DISCUSSION

Single-site synapses at interneuron–interneuron connections

Multivesicular release can be demonstrated at the level of spontaneous synaptic activity (Figs. 1, 2), where signals arise from several synaptic connections and where many connections involve several release sites. This approach has the advantage that it is readily applicable to any slice preparation. However, quantitative interpretation of the results is obviously much easier if experiments can be performed at single connections involving one release site. In another study, we present results from single-site interneuron–interneuron synapses using paired recordings (Kondo and Marty, 1998). Some of the results presented here (Fig. 9) were obtained with this technique. For the major part of the results, however, we took advantage of the flexibility of extracellular stimulation to select "simple" connections where successful responses can be grouped in a single peak. Furthermore, we showed that when the probability of release is decreased at these junctions, the position of the mean does not change markedly, and the CV usually does not increase. These experiments (Fig. 4) dismiss the possibility that the single peak histograms would arise from several sites with very high release probabilities (Silver et al., 1996). Taken together, the results provide convincing evidence that a fraction of interneuron–interneuron synapses ("simple" connections) involve a single functional release site. However, as already discussed in Auger and Marty (1997), it should be kept in mind that a single functional release site does not necessarily correspond to an anatomically defined single release site. Because cross-talk between neighboring sites

can occur for distances on the order of 1 μm or less (Clements, 1996; Barbour and Häusser, 1997), two closely apposed release sites with a separation of <1 μm could function as a single one. A recent electron microscopy study indicates that in interneurons of the molecular layer of the cerebellum, the density of GABAergic synapses on a given postsynaptic dendrite is low (Nusser et al., 1997). Some closely apposed sites were seen occasionally (Fig. 2*A*), but in the more general case synaptic contacts consisted of isolated release sites. This indicates that single functional sites are likely to correspond to single morphological release sites.

Evidence for multivesicular release at single release sites

The evidence indicating multivesicular release at single-site interneuron–interneuron synapses can be summarized as follows.

Event pairs with amplitude occlusion

This is the most direct evidence for multivesicular release. Event pairs with time intervals of <5 msec are observed in spontaneous synaptic currents, in single-site IPSCs obtained with extracellular stimulation, and in single-site IPSCs obtained in paired recordings. In all three experimental conditions, the frequency of these events is much higher than that expected from the superimposition of simple events with the randomly occurring background synaptic activity. A further argument against random superimposition of events is that the amplitudes of second events are on average markedly smaller than that of the preceding one. This phenomenon, amplitude occlusion, suggests that the first and second event in a pair share the same postsynaptic receptors. The finding of similar occupancy values for multiple events at single-sites synapses (0.70) and in α-latrotoxin-induced bursts (0.76) (Auger and Marty, 1997) is an important check of the internal consistency of our analysis. Finally it should be noted that the number of event pairs drops steeply as a function of time interval (Fig. 6*B*). The time constant of this decay cannot be determined precisely from our experiments, but it is of the same order of magnitude as that of the "driving function" derived from first latency histograms (~0.25 msec) (Fig. 10), as expected from a model where the release of several vesicles occurs independently of each other (Appendix 2).

Correlation between amplitude and kinetics

At single-site synapses, unresolved multivesicular events are expected to have larger amplitudes (because of incomplete receptor saturation by a single vesicle), slower rise times (because of jitter between the constituent elementary events), and slower decays (because of a more prolonged neurotransmitter concentration transient) than single events. Accordingly, the multivesicular release hypothesis predicts a positive correlation between amplitudes and rise times, and between amplitudes and decay times. Such correlations were found in single-site synapses both when using extracellular stimulation (results not shown) and in paired recordings (Kondo and Marty, 1998). These results are confirmed and further quantified by experiments such as that of Figure 8, which compare mean kinetics for single and multiple events at a single-site synapse.

Correlation between amplitudes and latencies

At single-site synapses, amplitudes are correlated to latencies as expected on the basis of multivesicular release and partial receptor saturation (Figs. 8–10; Appendix 2). A similar effect was described recently at what may have been a single-site pyramid–pyramid synapse in a cortical slice (Markram et al., 1997, their Fig. 3).

Separation of amplitude histograms between simple- and multiple-event components

In certain single-site amplitude histograms two components can be distinguished within the response peak (Fig. 7). The ratio between large and small amplitude levels is consistent with the notion that the small and large amplitude events correspond to single and multiple vesicular release, respectively.

Multivesicular synaptic currents have not been reported at single-site synapses before the present work. It is worth pointing out that in earlier publications (Gulyàs et al., 1993; Arancio et al., 1994; Silver et al., 1996) the quantal size is on the order of 10 pA, an order of magnitude smaller than in the present work. The large quantal size of interneuron synaptic currents is probably the key factor that allowed us to demonstrate multiquantal events.

Estimating the number of released vesicles at single sites

Because of the fast kinetics of vesicular release and of the high but incomplete occupancy of the postsynaptic receptors, most of the multivesicular release events were not detected as such. Therefore the proportion of doublets that was measured in single-site experiments (4.3%) must be considered an unrealistic lower estimate of the true proportion of multiple release events. Two methods can be used to obtain a better estimate of the proportion of multiple release. The most direct approach is to measure the proportion of smaller and larger events in the cases where two subpeaks were visible in the amplitude distributions. The proportion of multiple release obtained with this method, 30% on average, suggests that multiple release is in fact a quite prevalent phenomenon. The same conclusion can be drawn from the more elaborate analysis of latency–amplitude correlation plots (Figs. 9, 10). For the experiment shown in Figure 10, a proportion of 69% of multiple events can be calculated. It is likely that this number varies from one synaptic site to the next, as do other parameters describing basic properties of synaptic transmission (Auger and Marty, 1997; Nusser et al., 1997). We argued from the analysis of Figure 10 that when results are averaged across preparations, >27% of evoked IPSCs correspond to multivesicular release. Because the release probability increases steeply with temperature in slice preparations (Hardingham and Larkman, 1998), and because our experiments were performed at room temperature, the percentage of multivesicular events is likely higher at physiological temperature.

Fluctuations in the release probability function from trial to trial

We have considered two variants for the model of the release probability of synaptic vesicles. In one variant the probability is constant from trial to trial, and the numbers of vesicles released per trial follow a Poisson distribution. In the other variant the probability is allowed to drop to 0 for some of the trials, as would be expected, for example, if there were propagation failures. The second model was required to obtain a reasonable fit of the data in Figure 10. We stress, however, that the all-or-none alternation in release probability assumed for Figure 10 was chosen for the sake of simplicity; other schemes allowing more gradual fluctuations of the release probability are just as likely. Still other models, assuming for instance a process by which the release of a first vesicle would facilitate the release of another one, cannot be excluded. However, the suggestion that some of the synapses

exhibit variations in the release probability from trial to trial is attractive because it is in line with previous results obtained at interneuron–Purkinje cell synapses as well as at interneuron–interneuron synapses (Vincent and Marty, 1996; Kondo and Marty, 1998). Thus evidence is accumulating suggesting that quantal fluctuations are not the only determinant of variations in GABA release at interneuron terminals.

APPENDIX 1. AMPLITUDE DISTRIBUTION AT A SINGLE RELEASE SITE: COMBINING A POISSON DISTRIBUTION WITH PARTIAL RECEPTOR SATURATION

To model the pattern of release probability, we assume a very large pool of vesicles, each vesicle having a low probability of release. All vesicles have the same probability to undergo exocytosis, and there is no interaction between release events. The numbers of vesicles released for each trial follow the predictions of a Poisson distribution, such that the probability to observe 0 or j (>0) vesicles is respectively:

$$E(0) = \exp(-m)$$

$$E(j) = (m^j/j!)\exp(-m)$$

where m is the mean number of released vesicles. $E(0)$ is the observed number of failures, F, so that $m = -\ln(F)$.

A variant of the Poisson model assumes that the release probability is 0 for some of the trials and is constant ($p > 0$) for the others. Then the release can again be considered as a Poisson process for the cases where $p > 0$. The above equations then become:

$$E(j) = (m'^j/j!)\exp(-m'), \quad (1)$$

$$m' = -\ln(F'), \quad (2)$$

where m' and F', respectively, represent the mean number of released vesicles and the proportion of failures under the condition that $p > 0$.

The mean amplitudes of single, double, and multiple events can be calculated by assuming progressive saturation of a common set of postsynaptic receptors. We call ω the proportion of receptors occupied after one release event. After a first release with mean amplitude A_1, a second release event finds only a fraction $(1 - \omega)$ of the receptors that are free for activation. Because interevent intervals are very short (<3 msec) compared with the decay kinetics of the IPSCs, the partial recovery in the number of available receptors attributable to deactivation during the interval between the two events was neglected. Therefore the ratio of the amplitude increment for the second event over A_1 is $A'_2/A_1 = (1 - \omega)$. Because of poor event discrimination, most double-release events are detected as a single event with the total amplitude $A_2 = A_1 + A'_2$ (Auger and Marty, 1997). The ratio to the mean amplitude of truly single events is:

$$A_2/A_1 = 1 + (1 - \omega). \quad (3)$$

Likewise, after j consecutive release events the total amplitude is:

$$A_j = A_1(1 + (1 - \omega) + \ldots + (1 - \omega)^{j-1}) = A_1(1 - (1 - \omega)^j)/\omega. \quad (4)$$

The maximum of this expression, corresponding to very large values of j, is A_1/ω.

APPENDIX 2: PREDICTION OF AMPLITUDE–LATENCY CURVES

For this calculation the time span of the latency histogram (~2 msec) is fragmented into n δt increments, and we call $p(k)$ the probability to observe a release event during the time interval $[(k - 1)\,\delta t, k\,\delta t]$. Release events are assumed to be independent, so that $p(k)$ does not depend on whether events occurred before the kth interval. δt is small enough such that the probability to observe two events during one interval can be neglected. The sum of all values of $p(k)$ represents m, the mean number of vesicles released for one presynaptic action potential:

$$\sum_1^n p(k) = m. \quad (5)$$

Let $l(k)$ be the probability to observe a first latency in the $[(k - 1)\,\delta t, k\,\delta t]$ interval. $l(k)$ is the product of $p(k)$ with the probability that no event occurred until the kth interval, which is:

$$1 - \sum_1^{k-1} l(j).$$

Therefore:

$$p(k) = l(k)/(1 - \sum_1^{k-1} l(j)). \quad (6)$$

The sum of the $l(k)$ histogram represents the probability of observing at least one event after a presynaptic stimulus:

$$\sum_1^n l(k) = 1 - F, \quad (7)$$

where F represents the probability of failures.

We model l by an α function:

$$l(k) = Ck\delta t \exp(-k\delta t/\tau), \quad (8)$$

where τ is a time factor, and C is a constant, which is chosen such that Equation 7 is satisfied. Examples of time profiles of the functions $p(k)$ ("driving function") and $l(k)$ ("latency") calculated on the basis of Equations 6 and 8 are illustrated in the top panels of Figure 10.

To predict the mean amplitude of events having a first latency in the kth interval, we need to know the probability that additional vesicular release events will occur after the kth interval. The numbers of later release events follow a Poisson process with an expectation value:

$$m_k = \sum_{k+1}^{\infty} p(i). \quad (9)$$

Therefore the probabilities $V_j(k)$ to have j vesicles released after the kth time interval follow the relations:

$$V_0(k) = \exp(-m_k), \quad (10)$$

$$V_j(k) = (m_k^j/j!)\exp(-m_k). \quad (11)$$

Note that the same equations apply to the probabilities V_j to observe j release events over the entire latency distribution, that $m_0 = m$ and that $V_0 = \exp(-m) = F$.

The probability to obtain a total of j vesicles released with a first latency in the kth interval is:

$$P_j(k) = l(k)V_{j-1}(k). \quad (12)$$

At each time interval the mean current amplitude $A(k)$ is given by the proportion of events with 1, 2, . . . j vesicles such that:

$$A(k) = \sum_{j \geq 1} P_j(k)A_j. \quad (13)$$

These equations, together with Equation 4 allow calculation of the dependence of mean amplitude on latency, starting from the latency distribution and from the value of ω. If the probability of release is allowed to fluctuate among trials between $p(k)$ and 0, then the same equations apply, except that m and F should be replaced by m' and F', as explained in Appendix 1.

REFERENCES

Arancio O, Korn H, Gulyàs A, Freund T, Miles R (1994) Excitatory synaptic connections onto rat hippocampal inhibitory cells may involve a single transmitter release site. J Physiol (Lond) 481:395–405.

Auger C, Marty A (1997) Heterogeneity of functional synaptic parameters among single release sites. Neuron 19:139–150.

Barbour B, Häusser M (1997) Intersynaptic diffusion of neurotransmitter. Trends Neurosci 20:377–384.

Bekkers JM (1994) Quantal analysis of synaptic transmission in the central nervous system. Curr Opin Neurobiol 4:360–365.

Clements JD (1991) Quantal synaptic transmission? Nature 353:396.

Clements JD (1996) Transmitter timecourse in the synaptic cleft: its role in central synaptic function. Trends Neurosci 19:163–171.

Forti L, Bossi M, Bergamaschi A, Villa A, Malgaroli A (1997) Loose-patch recordings of single quanta at individual hippocampal synapses. Nature 388:874–878.

Frankenhaeuser B, Hodgkin AL (1957) The action of calcium on the electrical properties of squid axons. J Physiol (Lond) 137:218–244.

Galarreta M, Hestrin S (1997) Properties of $GABA_A$ receptors underlying inhibitory synaptic currents in neocortical pyramidal neurons. J Neurosci 17:7220–7227.

Gulyàs AI, Miles R, Sík A, Tóth K, Tamamaki N, Freund TF (1993) Hippocampal pyramidal cells excite inhibitory neurons through a single release site. Nature 366:683–687.

Hamann M, Attwell D (1996) Non-synaptic release of ATP by electrical stimulation in slices of rat hippocampus, cerebellum and habenula. Eur J Neurosci 8:1510–1515.

Hardingham NR, Larkman AU (1998) The reliability of excitatory synaptic transmission in slices of rat visual cortex in vitro is temperature dependent. J Physiol (Lond) 507:249–256.

Jones MV, Westbrook GL (1995) Desensitized states prolong GABAA channel responses to brief agonist pulses. Neuron 15:181–191.

Katz B (1969) The release of neural transmitter substances. The Sherrington Lectures. Liverpool, UK: Liverpool UP.

Kondo S, Marty A (1998) Synaptic currents at individual connections among stellate cells in rat cerebellar slices. J Physiol (Lond), 509:221–232.

Llano I, Gerschenfeld HM (1993) Inhibitory synaptic currents in stellate cells of rat cerebellar slices. J Physiol (Lond) 468:177–200.

Llano I, Marty A, Armstrong CM, Konnerth A (1991) Synaptic- and agonist-induced excitatory currents of Purkinje cells in rat cerebellar slices. J Physiol (Lond) 434:183–213.

Llano I, Tan YP, Caputo C (1997) Spatial heterogeneity of intracellular Ca2+ signals in axons of basket cells from rat cerebellar slices. J Physiol (Lond) 502:509–519.

Markram H, Lübke J, Frotscher M, Roth A, Sakmann B (1997) Physiology and anatomy of synaptic connections between thick tufted pyramidal neurones in the developing rat neocortex. J Physiol (Lond) 500:409–440.

Midtgaard J (1992) Membrane properties and synaptic responses of Golgi cells and stellate cells in the turtle cerebellum in vitro. J Physiol (Lond) 457:329–354.

Nusser Z, Cull-Candy SG, Farrant M (1997) Differences in synaptic Gaba(A) receptor number underlie variation in Gaba mini amplitude. Neuron 19:697–709.

Raastad M (1995) Extracellular activation of unitary excitatory synapses between hippocampal CA3 and CA1 pyramidal cells. Eur J Neurosci 7:1882–1888.

Raastad M, Storm JF, Andersen P (1992) Putative single quantum and single fiber excitatory postsynaptic currents show similar amplitude range and variability in rat hippocampal slices. Eur J Neurosci 4:113–117.

Redman S (1990) Quantal analysis of synaptic potentials in neurons of the central nervous system. Physiol Rev 70:165–198.

Scanziani M, Salin PA, Vogt KE, Malenka RC, Nicoll RA (1997) Use-dependent increases in glutamate concentration activate presynaptic metabotropic glutamate receptors. Nature 385:630–634.

Silver RA, Cull-Candy SG, Takahashi T (1996) Non-NMDA glutamate receptor occupancy and open probability at a rat cerebellar synapse with single and multiple release sites. J Physiol (Lond) 494:231–250.

Sotelo C, Llinas R (1972) Specialized membrane junctions between neurons in the vertebrate cerebellar cortex. J Cell Biol 53:271–289.

Tang CM, Margulis M, Shi QY, Fielding A (1994) Saturation of postsynaptic glutamate receptors after quantal release of transmitter. Neuron 13:1385–1393.

Tong G, Jahr CE (1994) Multivesicular release from excitatory synapses of cultured hippocampal neurons. Neuron 12:51–59.

Triller A, Korn H (1982) Transmission at a central inhibitory synapse. III. Ultrastructure of physiologically identified and stained terminals. J Neurophysiol 48:708–736.

Vincent P, Marty A (1993) Neighboring cerebellar Purkinje cells communicate via retrograde inhibition of common presynaptic interneurons. Neuron 11:885–893.

Vincent P, Marty A (1996) Fluctuations of inhibitory postsynaptic currents in Purkinje cells from rat cerebellar slices. J Physiol (Lond) 494:183–199.

Vincent P, Armstrong CM, Marty A (1992) Inhibitory synaptic currents in rat cerebellar Purkinje cells: modulation by postsynaptic depolarization. J Physiol (Lond) 456:453–471.